Lin *et al. Journal of Hematology & Oncology* (2025) 18:57
https://doi.org/10.1186/s13045-025-01712-3

Journal of
Hematology & Oncology

RESEARCH

Open Access

Engineered CRO-CD7 CAR-NK cells derived from pluripotent stem cells avoid fratricide and efficiently suppress human T-cell malignancies

Yunqing Lin[1,2†], Ziyun Xiao[1,2†], Fangxiao Hu[3], Xiujuan Zheng[1,2], Chenyuan Zhang[1,2], Yao Wang[1,2], Yanhong Liu[1,2], Dehao Huang[3], Zhiqian Wang[1,2], Chengxiang Xia[3], Qitong Weng[1,2], Leqiang Zhang[1,2], Yaoqin Zhao[1,2], Hanmeng Qi[3], Yiyuan Shen[3], Yi Chen[3], Fan Zhang[1,2], Jiaxin Wu[1,2], Pengcheng Liu[1,2], Jiacheng Xu[1,2], Lijuan Liu[1,2], Yanping Zhu[1,2], Jingliao Zhang[4], Wenbin Qian[5], Aibin Liang[6], Xiaofan Zhu[4], Tongjie Wang[1,2,3*], Mengyun Zhang[1,2,3*] and Jinyong Wang[1,2,3*]

Abstract

Background T-cell malignancies are highly aggressive hematological tumors with limited effective treatment options. CAR-NK cell therapy targeting CD7 has emerged as a promising approach for treating T-cell malignancies. However, conventional CAR-NK cell therapy faces the challenges of cell fratricide due to CD7 expression on both malignant cells and normal NK cells. Additionally, engineering CARs into human tissue-derived NK cells demonstrates heterogeneity, low transduction efficiency, and high manufacturing costs.

Methods The human pluripotent stem cells (hPSCs) were genetically modified by knocking out the *CD7* gene and introducing the CD7 CAR expression cassette to generate CD7 KO-CD7 CAR-hPSCs. These modified hPSCs were subsequently differentiated into CD7 KO-CD7 CAR-iNK cells using an efficient organoid induction method. The cytotoxicity of CD7 KO-CD7 CAR-iNK cells against $CD7^+$ tumor cells was evaluated. Furthermore, we overexpressed the *CXCR4* gene in CD7 KO-CD7 CAR-hPSCs and derived CXCR4-expressing CD7 KO-CD7 CAR-iNK (CRO-CD7 CAR-iNK) cells. The dynamics of CRO-CD7 CAR-iNK cells in vivo were tracked, and their therapeutic efficacy was assessed using human T-cell acute lymphoblastic leukemia (T-ALL) xenograft models.

Results The CD7 KO-CD7 CAR-iNK cells derived from CD7 KO-CD7 CAR-hPSCs effectively avoided fratricide, demonstrated normal expansion, and exhibited potent and specific anti-tumor activity against $CD7^+$ T-cell tumor cell lines and primary T-ALL cells. CXCR4 overexpression in CRO-CD7 CAR-iNK cells improved their homing capacity and extended their persistence in vivo. The CRO-CD7 CAR-iNK cells significantly suppressed tumor growth and prolonged the survival of T-ALL tumor-bearing mice.

†Yunqing Lin and Ziyun Xiao contributed equally to this work.

*Correspondence:
Tongjie Wang
wangtongjie@ioz.ac.cn
Mengyun Zhang
zhangmengyun@ioz.ac.cn
Jinyong Wang
wangjinyong@ioz.ac.cn
Full list of author information is available at the end of the article

Conclusions Our study provides a reliable strategy for the large-scale generation of fratricide-resistant CD7 CAR-iNK cells with robust anti-tumor effects from hPSCs, offering a promising cell product to treat T-cell malignancies.

Keywords Human pluripotent stem cells, CD7 CAR-NK, T-ALL, Fratricide-resistance, CXCR4, Persistence

Background

T-cell malignancies are a type of highly aggressive hematological malignancy. Adult patients with relapsed or refractory T-cell malignancies have poor disease outcomes with a 5-year overall survival rate lower than 20% [1–3]. Therefore, innovative therapies are needed for the treatment of T-cell malignancies. In recent years, chimeric antigen receptor (CAR)-T cell therapy targeting CD19 and BCMA has shown promising outcomes for relapsed or refractory B-cell malignancies and multiple myeloma [4, 5]. However, similar approaches to tackling T-cell malignancies have been more challenging because of the shared expression of many targetable antigens between normal and malignant T cells, which results in fratricidal effects during CAR-T cell production.

CD7 is a transmembrane glycoprotein mainly expressed by T cells, natural killer (NK) cells, and their precursors [6, 7]. It also serves as a crucial surface marker for tumor cells in hematological malignancies and is expressed in 95% of lymphoblastic T-cell leukemias and lymphomas, as well as in a subset of peripheral T-cell lymphomas [8]. Therefore, immunotherapy that targets CD7 is capable of covering the majority of T-cell malignancy subtypes. Currently, multiple CD7 CAR-T cell therapies for T-cell leukemia and T-cell lymphoma are undergoing clinical trials [9]. Some studies have demonstrated the impressive short-term efficacy of allogeneic donor-derived anti-CD7 CAR-T cells in an early-phase clinical trial involving patients with relapsed and/or refractory T-ALL [10, 11]. However, previous studies have reported that the expansion of CD7 CAR-T/CAR-NK cells was impaired due to fratricide, limiting their therapeutic potential [12]. To prevent fratricide in CAR-T and CAR-NK cells, strategies have been developed to remove the surface CD7 antigen through genome editing or an intracellular protein expression blocker [12–17].

CAR-NK cells exhibit comparable effector functions to CAR-T cells and have emerged as a promising immunotherapy option due to their minimal toxicities and universality [18]. CD7 CAR-NK therapy is expected to provide a safer and more universally applicable immunotherapy for the treatment of T-cell malignancies. Nevertheless, tissue-derived NK cells face several challenges, including functional heterogeneities, low efficiencies, and high costs of gene engineering or editing. Human pluripotent stem cells, including human embryonic stem cells (hESCs) and induced pluripotent stem cells (iPSCs), are promising cell sources to produce standardized, off-the-shelf NK cells, offering advantages such as unlimited cell sources and the ability to perform multiple genetic modifications. Leveraging these properties, hPSCs enable efficient genetic manipulation starting from small numbers of initial cells, thereby generating large quantities of gene-modified NK cells. It not only reduces the costs associated with engineering large numbers of NK cells but also ensures the gene-editing efficiency and homogeneity of the NK cell products. iPSCs can be prepared by reprogramming somatic cells from adults and enable personalized precision cell therapy without immunogenicity. hESCs, which are naturally derived pluripotent cells, demonstrate superior safety profiles and efficient differentiation ability [19]. However, the immunogenicity issue of allo-hESC-derivative cells is a challenge for universal applications. Currently, pre-engineered CAR-hPSC-induced CAR-NK (CAR-iNK) cells have been reported to exhibit promising anti-tumor activity against both hematological and certain solid tumors [20–23].

Current treatment strategies for T-cell malignancies have not demonstrated strong efficacy or long-term persistence of allogeneic CAR-NK cells after infusion [24]. Further efforts are required to enhance the therapeutic efficacy of CAR-NK therapy for T-cell malignancies. Studies have shown that ex vivo manipulation of NK cells results in the downregulation of CXCR4, which plays a crucial role in their homing to the bone marrow. Engineering strategies to stably equip effector NK cells with CXCR4 have shown promise in restoring their bone marrow homing ability and enhancing their cytotoxic capacities [25–30].

In this study, we verified that umbilical cord blood (UCB)-derived CD7 CAR-NK cells attacked autologous NK cells and showed an impaired expansion ability. To generate large-scale, fratricide-resistant CD7 CAR-iNK cells from hPSCs, we initially knocked out the *CD7* gene at the hPSC stage (CD7 KO-hPSCs) using CRISPR/Cas12 technology and subsequently differentiated these CD7 KO-hPSCs into CD7 knockout NK cells (CD7 KO-iNK). The CD7 KO-iNK cells successfully avoided the fratricidal effect of CD7 CAR-NK cells. Then we overexpressed CD7 CAR in the CD7 KO-hPSCs and differentiated them into CD7 CAR-expressing CD7 KO-iNK (CD7 KO-CD7 CAR-iNK) cells. These cells exhibited restored expansion capacity and efficiently eliminated $CD7^+$ T-cell tumor cell lines and primary T-ALL cells

in vitro. To further enhance the in vivo persistence and tumor-killing potential of CD7 KO-CD7 CAR-iNK cells, we ectopically expressed CXCR4 in CD7 KO-CD7 CAR-hPSCs (CRO-CD7 CAR-hPSCs). CRO-CD7 CAR-iNK cells, derived from CRO-CD7 CAR-hPSCs, exhibited prolonged persistence in vivo. The CRO-CD7 CAR-iNK cells significantly suppressed tumor growth and prolonged the survival of tumor-bearing mice. Therefore, we provided a reliable strategy for the large-scale generation of fratricide-resistant CRO-CD7 CAR-iNK cells with robust anti-tumor effects from hPSCs, offering a promising cell product to treat T-cell malignancies.

Methods

Mice

B-NDG (NOD.CB17-*Prkdc*^{scid}*Il2rg*^{tm1Bcgen}/Bcgen) and B-NDG hIL15 (NOD.CB17-*Prkdc*^{scid} *Il2rg*^{tm1Bcgen} *Il15*$^{tm1(IL15)Bcgen}$/Bcgen) mice were purchased from Biocytogen. Mice were housed in the SPF-grade animal facility of the Institute of Zoology, Chinese Academy of Sciences.

Cell culture

The hPSC line (Q380-human embryonic stem cell line) was provided by the National Stem Cell Resource Center, Institute of Zoology, Chinese Academy of Sciences. hPSC lines (CD7 KO-hPSCs, CD7 KO-CD7 CAR-hPSCs, CRO-CD7 CAR-hPSCs, CRO-CD7 CAR-luci-hPSCs, and CD7 KO-CD7 CAR-luci-hPSCs) were maintained in Essential 8 medium (Gibco) on vitronectin (Gibco) coated plates. The OP9 cell line was purchased from ATCC and cultured with α-MEM (Gibco) with 20% fetal bovine serum (FBS) (Ausbian). The differentiation of hPSCs into iNKs and the related anti-tumor activity assessments of iNK cells in animals are approved by the Biomedical Research Ethics Committee of the Institute of Zoology, Chinese Academy of Sciences. Jurkat and CCRF-CEM cell lines were purchased from MeisenCTCC and cultured with RPMI 1640 medium (Gibco) supplemented with 10% FBS. UCB samples were provided by Guangdong Umbilical Cord Blood Bank (Guangzhou, China). UCB-NK cells were cultured in KBM581 medium (Corning) supplemented with rhIL-2 (Recombinant human interleukin-2, 200 IU/mL, Miltenyi) and SGR-SM (1%, DAKEWE). The primary T-ALL cells used in this study were from the Institute of Hematology and Blood Diseases Hospital, Chinese Academy of Medical Sciences and Peking Union Medical College with the donors'informed consent.

Retrovirus packaging

The monospecific CAR constructs included an immunoglobulin heavy chain signal peptide (SP), an anti-CD7 single-chain variable fragment (scFv) (CD7 scFv:TH-69) [31], a CD8α hinge domain, a transmembrane domain (TMD) of CD8α, and a signaling domain (SD) of CD3ζ. The EGFP coding sequence and CAR constructs (CD7 scFv-CD8α Hinge-CD8α TMD-CD3ζ) were cloned into SFG recombinant retroviral vectors [32]. Retroviruses carrying the CAR vectors were generated as previously described [33].

Isolation of UCB-NK cells and generation of EGFP$^+$ Ctrl-NK and CD7 CAR-NK cells

CD3$^-$ UCB mononuclear cells purified using CD3 biotin (Biolegend) and the Anti-biotin MicroBeads UltraPure kit (Miltenyi Biotec) were stimulated on day 0 with K562-mIL-21 cells (Hangzhou Zhongying Biomedical Technology Co., Ltd.) and rhIL-2 in KBM581 serum-free medium. On day 0, activated NK cells were transduced with retroviral supernatants at a multiplicity of infection (MOI) of 5, following the Vectofusin-1 (Miltenyi Biotec) based transduction protocol. Infection rates of NK cells were assessed by flow cytometry on day 2. The EGFP$^+$ Ctrl-NK and CD7 CAR-NK cells were sorted and expanded for 12 days without being stimulated by K562-mIL-21 cells (Hangzhou Zhongying Biomedical Technology Co., Ltd).

Flow cytometry

Cells were blocked by Human TruStain FcX™ (Biolegend, 422302) antibody, and subsequently labeled with specific antibodies. The following antibodies or fluorescence labeled proteins were used: CD45 (Biolegend, HI30), CD3 (Biolegend, HIT3a), CD16 (Biolegend, 3G8), CD56 (Biolegend, HCD56), CD7 (Biolegend, 4H9/CD7), DNAM-1(Biolegend, 11A8), NKp30 (Biolegend, P30-15), NKp44 (Biolegend, P44-8), NKG2A (Biolegend, S19004C), CD94 (BD Biosciences, HP-3D9), CD69 (Biolegend, FN50), CD96 (Biolegend, NK92.39), CD319 (Biolegend, 162.1), TRAIL (Biolegend, RIK-2), GzmB (Biolegend, GB11), Perforin (Biolegend, dG9), CD184/CXCR4 (Biolegend, 12G5), Myc-Tag (Cell signaling technology, 9B11), APC-labeled and FITC-labeled Human CD7 Protein (Acro Biosystems, CD7-HF2H6). The cells were resuspended in the DAPI (Sigma-Aldrich) solution and analyzed with BD LSRFortessa X-20 cytometer (BD Biosciences). Flow cytometry data were analyzed by the FlowJo software (Tree Star, Ashland OR).

CRISPR/Cas12i-mediated CD7 knockout in hPSCs

Two sgRNA sequences, sgRNA1 (ggccgctgctttgggaggaagaa) and sgRNA2 (ttactacgaggacggggtggtgc), targeting intron 1 and exon 2 of CD7 respectively, were designed using a web-based guide-RNA designer (http://www.rgenome.net/) and subsequently cloned into the CRISPR/Cas12i expression vector (a gift from Dr. Wei Li of the Institute of Zoology, Chinese Academy of Sciences) [34].

To create CD7 knockout hPSCs (CD7 KO-hPSCs), the two sgRNA expression vectors were co-transfected into hPSCs using electroporation (Celetrix). Single-cell clones of hPSCs were harvested for DNA extraction using the TIANamp Genomic DNA kit (TIANGEN). The CD7 locus target sequences were amplified with the 2× Rapid Taq Master Mix (Vazyme) and the primer pairs depicted in Fig. S1D-E.

Plasmid construction and electroporation

The scFv specific for CD7 was used for CAR construction (CD7 scFv-CD8α Hinge-CD8α TMD-CD3ζ). The CAR construct was cloned into the PiggyBac expression vector (SBI) to generate the PiggyBac-EF1α-CD7 CAR vector (Table S1). The CD7 CAR PiggyBac vectors were then transduced into the CD7 KO-hPSCs by electroporation. Seven days after transduction, hPSCs were stained with FITC-labeled Human CD7 Protein, and sorted by BD FACSAria™ Fusion for two rounds to establish the stable CD7 CAR-expressing CD7 KO-hPSCs (CD7 KO-CD7 CAR-hPSCs). The cDNA sequences encoding the CXCR4 or luciferase were respectively cloned into the PiggyBac expression vector (Table S1). Then the CD7 KO-CD7 CAR-luci-hPSCs, CRO-CD7 CAR-hPSCs, and CRO-CD7 CAR-luci-hPSCs were constructed by two rounds of sorting following electroporation with the CXCR4 or luciferase-expressing vector.

Generation of Ctrl-iNK, CD7 KO-iNK, CD7 KO-CD7 CAR-iNK, CD7 KO-CD7 CAR-luci-iNK, CRO-CD7 CAR-iNK, and CRO-CD7 CAR-luci-iNK cells

The derivation of iNK cells from hPSCs has been previously described [35]. First, the hPSCs, CD7 KO-hPSCs, CD7 KO-CD7 CAR-hPSCs, CD7 KO-CD7 CAR-luci-hPSCs, CRO-CD7 CAR-hPSCs, and CRO-CD7 CAR-luci-hPSCs were subjected to a two-day monolayer induction to acquire highly purified lateral plate mesoderm cells. Subsequently, 2×10^4 lateral plate mesoderm cells and 5×10^5 OP9 feeder cells (GFP^+) were assembled into organoid aggregates and seeded onto a transwell insert for iNK induction. The organoids were plated on a 0.4 μm Millicell transwell insert (Corning) and placed in 6-well plates containing 1 mL hematopoietic differentiation medium per well [35]. The medium was changed completely every 2–3 days for two weeks. On day 16, the medium was changed to NK differentiation medium [36]. Half medium exchanges were performed every 2 days. On day 27, the mature Ctrl-iNK, CD7 KO-iNK, CD7 KO-CD7 CAR-iNK, CD7 KO-CD7 CAR-luci-iNK, CRO-CD7 CAR-iNK, and CRO-CD7 CAR-luci-iNK cells were harvested.

Cytotoxicity assays in vitro

CD7 KO-CD7 CAR-iNK cells or Ctrl-iNK cells (Effector, E) were cocultured with Jurkat or CCRF-CEM tumor cell lines (Target, T) labeled with Cell Proliferation Dye eFluor™ 670 (Invitrogen) in 96-well plates for 4 h at the indicated effector:target ratio (E:T ratio). In the serial target cytotoxic killing assay, effector cells were incubated with target cells for 1, 2, and 3 rounds respectively. The cell lysis ratio of eFluor™ 670 labeled target cells was detected. In the first round, effector cells were cocultured with eFluor™ 670 labeled target cells (Jurkat/CCRF-CEM) for 12 h at an E:T ratio of 1:1, respectively. In the second round, effector cells (CD7 KO-CD7 CAR-iNK/Ctrl-iNK) were cocultured with target cells (Jurkat/CCRF-CEM) for 12 h (E:T ratio = 1:1), and then an equal number of eFluor™ 670 labeled target cells (Jurkat/CCRF-CEM) were added to coculture for additional 12 h. In the third round, effector cells (CD7 KO-CD7 CAR-iNK/Ctrl-iNK) were cocultured with target cells (Jurkat/CCRF-CEM) for 12 h (E:T ratio = 1:1). Then, an equal number of target cells were added and cocultured for 12 h, followed by the coculture of eFluor™ 670 labeled target cells for an additional 12 h. Target cell death was assessed with a flow cytometer (BD LSRFortessa X-20 cytometer, BD Biosciences) by the percentage of DAPI positive cells in the eFluor™ 670-positive population. Flow cytometry data were analyzed by the FlowJo software (Tree Star, Ashland OR).

The primary T-ALL tumor cells were transplanted into B-NDG immunodeficient mice (1×10^6/mouse) via tail vein injection. Once the proportion of primary tumor cells exceeded 80% in the peripheral blood (PB) through weekly flow cytometry analysis, the spleens of the B-NDG recipient mice were harvested and lysed in ACK lysis buffer (Gibco). The cells were filtered through a 70 μm filter (BIologix) to obtain a single-cell suspension for the cytotoxicity assay. Effector cells (CD7 KO-CD7 CAR-iNK/Ctrl-iNK) were cocultured with primary T-ALL tumor cells labeled with eFluor™ 670 for 6 h at the indicated E:T ratios. Besides, the effector cells (CD7 KO-CD7 CAR-iNK/Ctrl-iNK) were also cocultured with primary T-ALL tumor cells labeled with eFluor™ 670 for 3, 6, 9, 12 h at an E:T ratio of 1:2.

PBMCs were purchased from SCHBIO Inc (Shanghai, China). CD7 KO-CD7 CAR-iNK cells or Ctrl-iNK cells were cocultured with PBMCs labeled with Cell Proliferation Dye eFluor™ 670 (Invitrogen) in 96-well plates for 6 h at the indicated E:T ratio.

Assessment of CD107a, TNF-α, and IFN-γ by flow cytometry

Ctrl-iNK or CD7 KO-CD7 CAR-iNK cells were cocultured with tumor cells (Jurkat or CCRF-CEM) at an

E:T ratio of 1:1 for 4 h to evaluate CD107a expression. After incubation, cells were stained with antibodies against CD56 and CD107a (H4A3, Biolegend). To evaluate TNF-α and IFN-γ expression, Ctrl-iNK or CD7 KO-CD7 CAR-iNK cells were cocultured with tumor cells (Jurkat or CCRF-CEM) at an E:T ratio of 1:1 for 2 h, followed by the addition of BFA/Monensin (MULTISCIENCES) and an additional 2-h incubation. After incubation, cells were stained with antibodies against CD56. FIX & PERM Kit (MULTISCIENCES) was used for fixation and permeabilization, followed by intracellular staining for TNF-α (Biolegend, MAb11) or IFN-γ (Biolegend, 4S.B3). The cells were analyzed with BD LSRFortessa X-20 cytometer (BD Biosciences). Data were analyzed using FlowJo software.

iNK cell tracking in vivo

CD7 KO-CD7 CAR-luci-iNK and CRO-CD7 CAR-luci-iNK cells (1×10^7 cells/mouse) were injected into the tail vein of the B-NDG hIL15 mice. Bioluminescence imaging (BLI, IVIS Spectrum PerkinElmer) was performed on the indicated days to trace and quantify the CD7 KO-CD7 CAR-luci-iNK and CRO-CD7 CAR-luci-iNK cells in each group of mice. Living image software (PerkinElmer) was used to visualize and calculate total luminescence. PB cells and bone marrow cells obtained from mice were lysed in ACK lysis buffer (Gibco, cat. no. A1049201), and human cell engraftment was assessed by flow cytometry. Spines were isolated for ex vivo imaging using BLI (IVIS Spectrum PerkinElmer).

T-ALL xenograft models with CRO-CD7 CAR-iNK cell treatment

Seven-to-eight-week-old B-NDG hIL15 mice were intravenously injected with the luciferase-expressing CCRF-CEM cells (1×10^5 cells/mouse) on day 0 to construct the T-ALL xenograft animal models. These models were irradiated (1.0 Gy, Rad Source RS2000) on day 1. Then, the mice were intravenously injected with an equal volume of PBS (200 μL), Ctrl-iNK (1×10^7 cells/mouse), CD7 KO-CD7 CAR-iNK (1×10^7 cells/mouse), and CRO-CD7 CAR-iNK (1×10^7 cells/mouse) cells on day 1, day 4, and day 7, respectively. BLI was performed every week to determine tumor aggressiveness. Mice suffering from heavy tumor burden were euthanized for ethical considerations. All animal experiments were conducted under the approval of the Institutional Animal Care and Use Committee (IACUC) of the Institute of Zoology of the Chinese Academy of Sciences (IOZ-2021-182).

Vector copy number analysis of CD7 CAR in CD7 KO-CD7 CAR-iNK cells and CRO-CD7 CAR-iNK cells

The genomic DNA of CD7 KO-CD7 CAR-iNK and CRO-CD7 CAR-iNK cells was extracted using the TIANamp Genomic DNA Kit (TIANGEN, cat. no. DP304). The primers were designed to amplify a 148-bp fragment spanning part of the CD8 hinge region and part of CD8 transmembrane region (Forward primer: 5'-ACCACT ACTCCCGCTCCAAGGC-3', Reverse primer: 5'-GAT CACGAGTGAAAGCAGCAGGACC-3', Probe: 5'-FAM-ACCATCGCCTCTCAGCCGCTTTCCC-TAMRA-3'). PiggyBac-EF1α-CD7 CAR vector (1×10^9 copies/μL) was used as the standard sample. A seven-point standard curve that consisted of 5×10^1 to 5×10^7 copies/μL of PiggyBac-EF1α-CD7 CAR vector was prepared. Quantitative real-time PCR was performed with 40 ng of genomic DNA in each reaction using Hieff Unicon® qPCR TaqMan Probe Master Mix (YEASEN, cat. no. 11205ES08), in a Real-Time PCR System (BIO-RAD, CFX Opus 96). The copy number was calculated as previously reported [37].

Statistical analysis

All quantitative analyses were performed with SPSS (IBM SPSS Statistics 25). All data are represented as mean ± SD, and the specific number (n) for each dataset is detailed in the figure legends. The two-tailed independent *t*-test, one-way ANOVA, two-way ANOVA, and Mann-Whitney U test were used to compare groups. Significance was defined as a *P* value of less than 0.05. Survival curves for tumor-bearing models were plotted using the Kaplan-Meier method and compared between groups using the logarithmic rank (Mantel-Cox) test. Statistical analysis was performed using the GraphPad Prism 9 software.

Results

Deletion of the CD7 gene enables iNK cells derived from hPSCs to avoid fratricide

To evaluate whether CD7 CAR expression in NK cells causes fratricide, we produced CD7 CAR-NK cells from UCB and assessed their cytotoxicity against NK cells (Fig. 1A). $CD3^-$ cells were isolated from the UCB mononuclear cells and expanded for six days. Flow cytometry analysis confirmed that 99.6% of the expanded NK cells expressed CD7 (Fig. S1A). The expanded NK cells were transduced with CD7 CAR retrovirus using spin infection. The expression of CD7 CAR was assessed by flow cytometry two days after retroviral infection, revealing an infection rate of over 90% (Fig. 1B). The CD7 CAR-NK cells were then cocultured with autologous uninfected NK cells derived from the same UCB

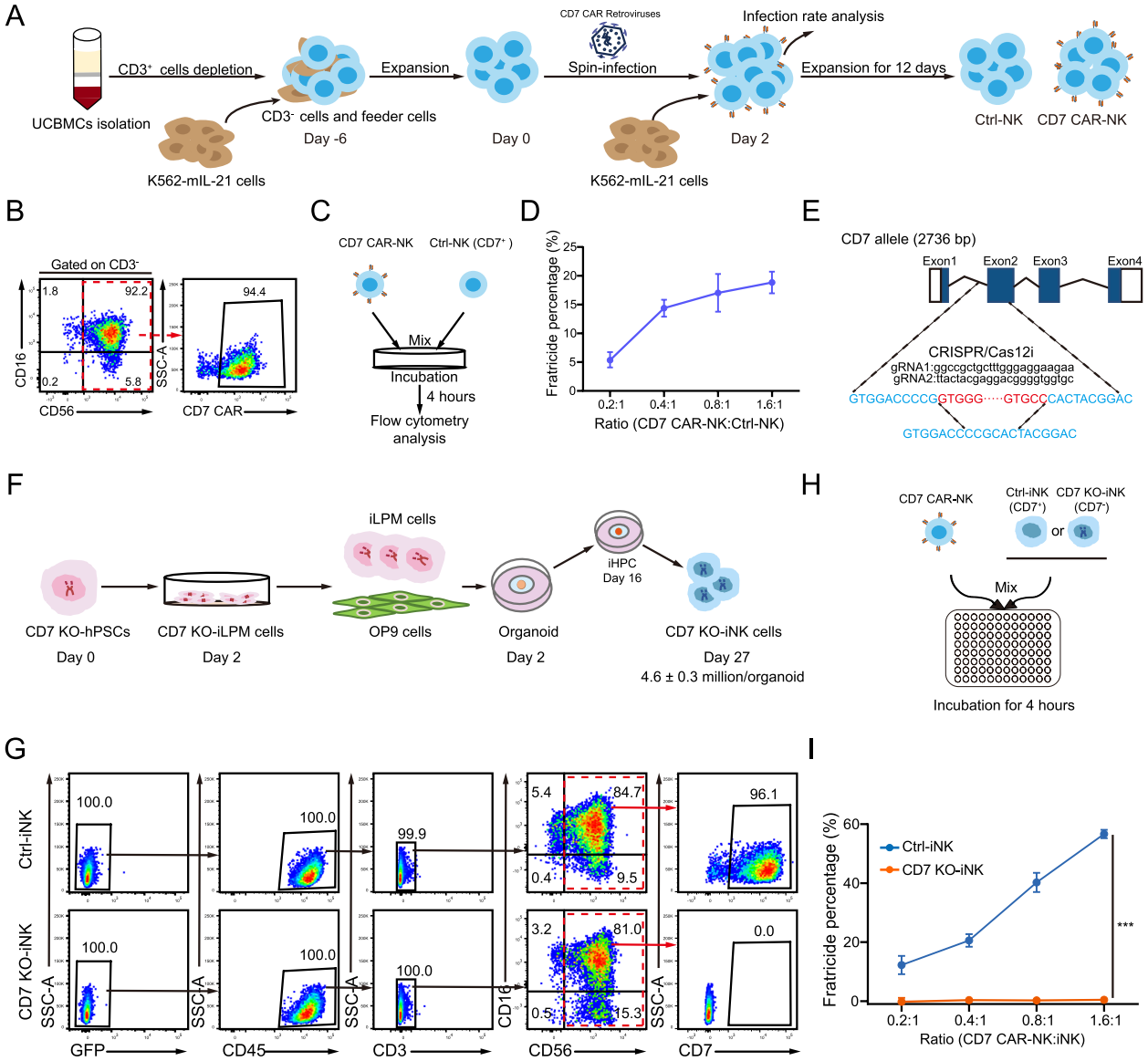

Fig. 1 hPSC-derived iNK cells lacking CD7 expression avoid fratricide. **A** Schematic diagram showing the generation of CD7 CAR-NK cells from UCB. **B** Flow cytometry analysis showing the infection rate of CD7 CAR in $CD3^{-}CD56^{+}$ NK cells. The infection rate was analyzed 48 h after transduction. **C** Schematic diagram of evaluating the cell lysis ratios of UCB-derived Ctrl-NK cells (uninfected with retrovirus) cocultured with CD7 CAR-NK cells. **D** Statistical analysis of the fratricide percentage of CD7 CAR-NK cells against Ctrl-NK cells at indicated E:T ratios (mean ± SD). $n = 4$ repeats. **E** Strategy for the knockout of *CD7* gene in hPSCs. The exons of the *CD7* gene are shown as blue boxes. Two gRNA sequences, gRNA1 and gRNA2, are shown in black. The deleted sequences are marked in red, and the sequences after editing are marked in blue. **F** Schematic diagram of CD7 KO-iNK cell induction. **G** Representative flow cytometry plots of CD7 KO-iNK cells ($GFP^{-}CD45^{+}CD3^{-}CD56^{+}CD16^{\pm}CD7^{-}$) on day 27. **H** Schematic diagram of evaluating the in vitro cytotoxic activity of CD7 CAR-NK cells against Ctrl-iNK cells or CD7 KO-iNK cells. **I** Statistical analysis of the fratricide percentage of CD7 CAR-NK cells against Ctrl-iNK cells or CD7 KO-iNK cells at indicated E:T ratios (two-way ANOVA, mean ± SD). $n = 4$ repeats. ***$p < 0.001$

sample to evaluate their fratricide effect (Fig. 1C). The results demonstrated that CD7 CAR-NK cells effectively killed $CD7^{+}$ NK cells (Fig. 1D). Furthermore, we constructed the $EGFP^{+}$ Ctrl-NK cells by transducing the expanded NK cells with the EGFP retrovirus (Fig. S1B). In contrast to $EGFP^{+}$ Ctrl-NK cells, the CD7 CAR-NK cells showed poor cell viability after 3 and 6 days of culture, confirming the existence of fratricide (Fig. S1C). Therefore, disrupting the surface expression of CD7 on NK cells to overcome fratricide was necessary for the production of clinical-scale CD7 CAR-NK cells. Previously, we developed an organoid

induction method for generating NK (iNK) and CAR-iNK cells from hPSCs [22, 23, 35]. In this study, we aimed to generate CD7 CAR-iNK cells from hPSCs using this reliable scale-up method. Given the fratricide in CD7 CAR-iNK cells, we first knocked out the *CD7* gene in hPSCs using CRISPR/Cas12i gene editing. Two gRNAs were designed to target sequences within the first intron and the second exon of the *CD7* gene (Fig. 1E). Genome PCR confirmed the deletion of the *CD7* gene in the hPSCs (Fig. S1D-F), indicating that we had successfully obtained CD7 KO-hPSCs. CD7 KO-iNK cells were further generated from CD7 KO-hPSCs. The unmodified hPSCs were used as controls to monitor any disruptions in differentiation caused by genetic modification. Briefly, the lateral plate mesoderm cells with CD7 KO (CD7 KO-iLPM) were efficiently induced from CD7 KO-hPSCs after two days of monolayer induction. On day 2, the CD7 KO-iLPM and OP9 cells were mixed to prepare organoid aggregates. The organoids were plated into the transwell for 25-day NK cell induction (Fig. 1F). On average, one unmodified hPSC or CD7 KO-hPSC could output 4.97 ± 0.21 (mean ± SD) Ctrl-iLPM or 5.1 ± 0.15 (mean ± SD) CD7 KO-iLPM (Fig. S1G). The generated Ctrl-iLPM could further differentiate into 1119.2 ± 44.0 (mean ± SD) Ctrl-iNK cells, and the generated CD7 KO-iLPM could further differentiate into 1144.2 ± 72.9 (mean ± SD) CD7 KO-iNK cells (Fig. S1H). More than 90% of resulting cells exhibited mature NK cell phenotypes ($GFP^-CD45^+CD3^-CD56^+CD16^\pm$) on day 27. Over 96% of Ctrl-iNK cells expressed CD7, while CD7 KO-iNK cells showed no CD7 expression (Fig. 1G). Flow cytometry analysis confirmed the absence of CD7 expression in CD7 KO-iNK cells. Notably, the GFP^+ cells were undetectable on day 27, demonstrating the absence of OP9 contamination in the iNK cells. To determine whether CD7 KO-iNK cells could avoid fratricide effect, Ctrl-iNK and CD7 KO-iNK cells were cocultured with UCB-derived CD7 CAR-NK cells (Fig. 1H). As expected, CD7 KO-iNK cells avoided CD7 CAR-NK cell-mediated cytotoxicity, whereas Ctrl-iNK cells, which expressed CD7, were significantly killed (Fig. 1I). Therefore, deletion of the *CD7* gene enables iNK cells to avoid attacks by CD7 CAR-NK cells.

Disruption of CD7 expression restores the expansion of CD7 CAR-iNK cells

Due to antigen-driven fratricide, UCB-derived CD7 CAR-NK cells exhibited poor expansion ability compared to the untransduced NK cells (Fig. 2A). To achieve expandable and functional CD7 CAR-iNK cells from hPSCs, we engineered the CD7 CAR expression cassette into CD7 KO-hPSCs to construct the CD7 CAR-expressing CD7 KO-hPSCs (CD7 KO-CD7 CAR-hPSCs) (Fig. 2B). The expression rates of CD7 CAR reached over 99% in CD7 KO-CD7 CAR-hPSCs after two rounds of sorting (Fig. S2A). CD7 KO-CD7 CAR-hPSCs were further differentiated into CD7 KO-CD7 CAR-iNK cells using the organoid induction method. Flow cytometry analysis showed that over 90% of CD7 KO-CD7 CAR-iNK cells expressed CD7 CAR while lacking CD7 expression (Fig. 2C). The CD7 KO-CD7 CAR-iNK cells demonstrated comparable expansion folds to Ctrl-iNK cells, indicating that the deletion of CD7 successfully restored expansion capacity in CD7 CAR-iNK cells (Fig. 2D). Furthermore, we assessed the expression of the crucial effector molecules in CD7 KO-CD7 CAR-iNK cells, including activating and inhibitory receptors (NKp30, NKp44, CD319, DNAM-1, CD96, NKG2A, and CD94), activating molecule (CD69), apoptosis-related ligands (TRAIL), and cytotoxic granules (GzmB and Perforin) (Fig. 2E). The expression levels of these molecules were similar among Ctrl-iNK, CD7 KO-iNK, and CD7 KO-CD7 CAR-iNK cells. The CD7 KO-CD7 CAR-iNK cells were cocultured with UCB-NK, Ctrl-iNK, and CD7 KO-iNK cells to verify whether fratricide exists in the CD7 KO-CD7 CAR-iNK cells (Fig. 2F). The results demonstrated that CD7 KO-CD7 CAR-iNK cells exerted strong cytotoxic activity against UCB-NK and Ctrl-iNK cells but exhibited no cytotoxicity against CD7 KO-iNK cells (Fig. 2G). Taken together, we successfully generate expandable and fratricide-resistant CD7 KO-CD7 CAR-iNK cells from CD7 KO-CD7 CAR-hPSCs.

(See figure on next page.)

Fig. 2 Disruption of CD7 expression restores the expansion of CD7 CAR-iNK cells. **A** Statistics analysis of the expansion folds of NK cells and CD7 CAR-NK cells derived from UCB on indicated expansion days (two-tailed independent *t*-test, mean ± SD). $n = 3$ repeats. NS, not significant ($p > 0.05$), *$p < 0.05$, **$p < 0.01$. **B** Strategy diagram for the acquisition of CD7 KO-CD7 CAR-iNK cells and the detection of their expansion capacity and cytotoxic activity. **C** Representative flow cytometry plots of Ctrl-iNK, CD7 KO-iNK, and CD7 KO-CD7 CAR-iNK cells ($GFP^-CD45^+CD3^-CD56^+CD16^\pm CD7^-$CD7 CAR^+) on day 27. **D** Statistics analysis of the expansion folds of Ctrl-iNK cells, CD7 KO-iNK cells, and CD7 KO-CD7 CAR-iNK cells on indicated expansion days (one-way ANOVA with Tukey's multiple-comparison test). $n = 3$ repeats. NS, not significant ($p > 0.05$). **E** Flow cytometry histograms showing the expression levels of NKp30, NKp44, CD319, DNAM-1, CD96, NKG2A, CD94, CD69, TRAIL GzmB, and Perforin in Ctrl-iNK, CD7 KO-iNK, and CD7 KO-CD7 CAR-iNK cells. **F** Schematic diagram of evaluating the in vitro cytotoxic activity of CD7 KO-CD7 CAR-iNK cells against UCB-NK, Ctrl-iNK, and CD7 KO-iNK cells. **G** Statistical analysis of the cytotoxic activity of CD7 KO-CD7 CAR-iNK cells against UCB-NK, Ctrl-iNK, and CD7 KO-iNK cells at an E:T ratio of 1:1 (one-way ANOVA with Tukey's multiple-comparison test). $n = 4$ repeats. ***$p < 0.001$

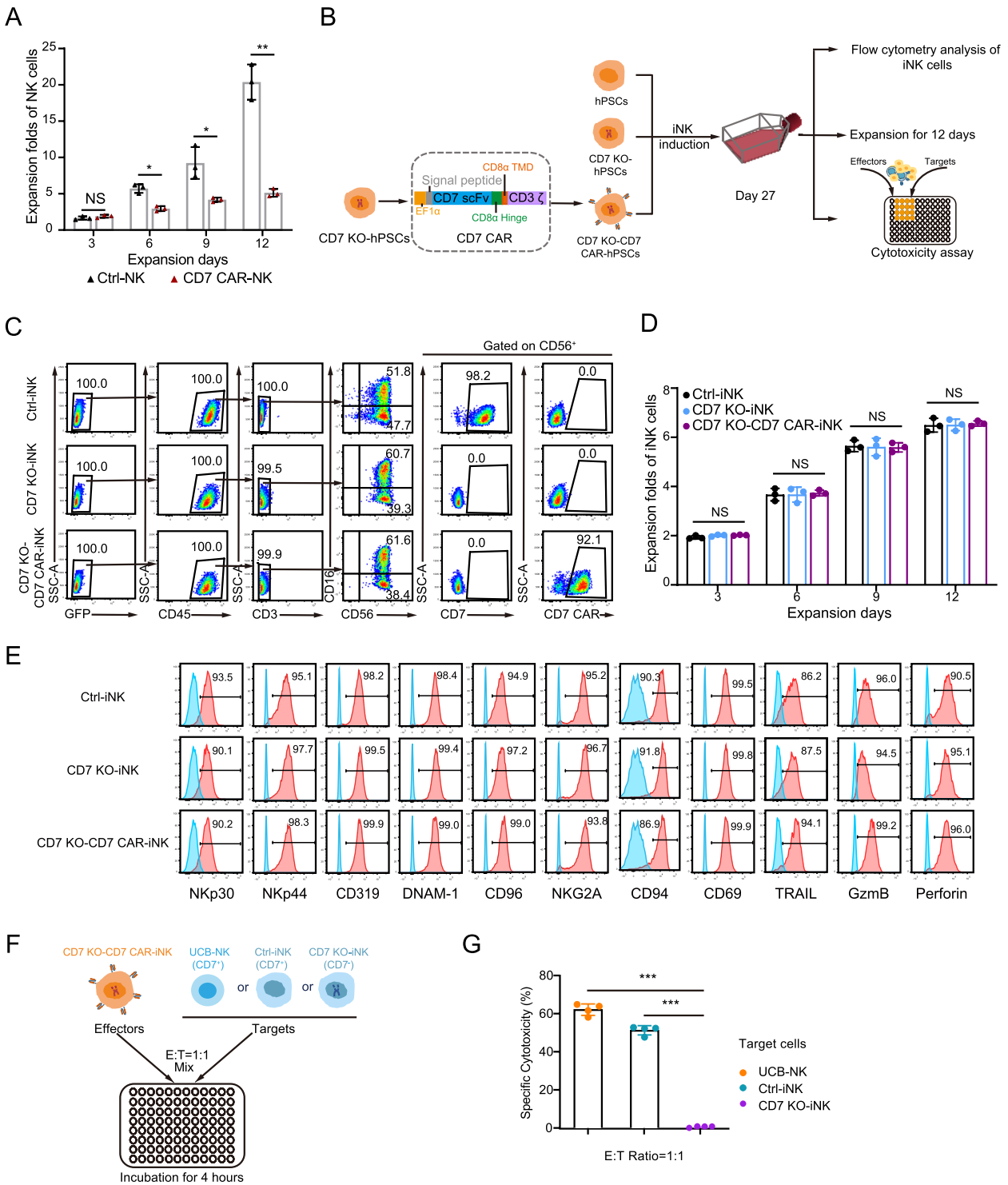

Fig. 2 (See legend on previous page.)

CD7 KO-CD7 CAR-iNK cells show robust tumor-killing abilities in vitro

We subsequently performed tumor-killing assays to evaluate the cytotoxicity of CD7 KO-CD7 CAR-iNK cells against T-ALL cells. The Jurkat and CCRF-CEM cells, which both highly expressed CD7 protein (Fig. S2B), were used as targets for the specific cytotoxicity assay. Tumor cells (targets, T) were cocultured with either Ctrl-iNK

cells or CD7 KO-CD7 CAR-iNK cells (effectors, E) at various E:T ratios (Fig. 3A). As expected, CD7 KO-CD7 CAR-iNK cells efficiently targeted and induced apoptosis in Jurkat and CCRF-CEM cells within 4 h, exhibiting significantly higher cytotoxicity compared to Ctrl-iNK cells (Fig. 3B and C, Fig. S2C and D). To further assess the persistent cytotoxicity of CD7 KO-CD7 CAR-iNK cells in serial cytotoxic killing assays, we conducted three rounds of tumor killing assays with Jurkat or CCRF-CEM cells (E:T = 1:1) (Fig. 3D). The results indicated that CD7 KO-CD7 CAR-iNK cells demonstrated a robust serial tumor-killing activity that was superior to that of Ctrl-iNK cells (Fig. 3E and F, Fig. S2E and F). Then, NK cell stimulation assays were conducted by coculturing CD7 KO-CD7 CAR-iNK cells with Jurkat or CCRF-CEM cells at an E:T ratio of 1:1 for 4 h. The expression of CD107a, a membrane protein associated with NK cell cytotoxic activity, and that of IFN-γ and TNF-α, NK cell cytotoxicity-related cytokines, was analyzed after incubation. As expected, the expression of CD107a in CD7 KO-CD7 CAR-iNK cells was significantly higher than that observed in Ctrl-iNK cells, indicating that CD7 KO-CD7 CAR-iNK cells released more cytotoxic granules (Fig. 3G and H, Fig. S2G). Meanwhile, CD7 KO-CD7 CAR-iNK cells exhibited elevated production of IFN-γ and TNF-α compared to Ctrl-iNK cells when stimulated with tumor cells (Fig. 3I-L, Fig. S2H and I). These results demonstrate the specific cytotoxic efficacy of CD7 KO-CD7 CAR-iNK cells.

CD7 KO-CD7 CAR-iNK cells exhibit anti-tumor activity against CD7$^+$ primary T-ALL cells

In addition to tumor cell lines, the cytotoxic potential of CD7 KO-CD7 CAR-iNK cells against primary T-ALL tumor cells was further evaluated. Freshly isolated mononuclear leukocytes from the bone marrow of three T-ALL patients were separately transplanted into B-NDG immunodeficient mice. Tumor progression was monitored weekly by analyzing the percentage of human CD45$^+$CD7$^+$ (huCD45$^+$CD7$^+$) tumor cells in PB using flow cytometry, starting four weeks after transplantation. Mice were sacrificed when the proportion of circulating huCD45$^+$CD7$^+$ cells exceeded 80% of the total PB mononuclear cell population. Subsequently, spleens from the B-NDG mice were harvested, processed into single-cell suspensions, and cocultured with iNK cells (Fig. 4A). Six to nine weeks after transplantation, cells were obtained from the spleens of B-NDG immunodeficient mice in which huCD45$^+$CD7$^+$ cells in the PB reached over 80% (Fig. S3A). These cells were then stained to check CD7 expression. All samples showed nearly 100% of CD7$^+$ cells (Fig. 4B). These tumor cells obtained from the spleens were then cocultured with CD7 KO-CD7 CAR-iNK and Ctrl-iNK cells at defined E:T ratios. The results demonstrated that CD7 KO-CD7 CAR-iNK cells effectively targeted and eliminated primary T-ALL cells from all three patients (Fig. 4C-E, Fig. S3B-D). Furthermore, the lysis of T-ALL tumor cells gradually increased over time, indicating the durable cytotoxicity of CD7 KO-CD7 CAR-iNK cells (Fig. 4F-H). When the CD7 KO-CD7 CAR-iNK cells were cocultured with T-ALL cells at a 1:2 ratio, approximately 93.5%, 86.5%, and 64.5% of T-ALL cells from patient 1, patient 2, and patient 3 were eradicated within 12 h, highlighting the potent effector function of the CD7 KO-CD7 CAR-iNK against primary tumors.

(See figure on next page.)

Fig. 3 The cytotoxic activity of CD7 KO-CD7 CAR-iNK cells against CD7$^+$ tumor cell lines in vitro. **A** Experimental design for the tumor-killing assay. The Ctrl-iNK and CD7 KO-CD7 CAR-iNK cells (effectors, E) were cocultured with Jurkat or CCRF-CEM tumor cells labeled with eFluor™ 670 (targets, T), respectively. The E:T ratios include 0.05:1, 0.1:1, 0.2:1, 0.4:1, 0.8:1, 1.6:1, 3.2:1, and 5:1. **B-C** Cytotoxicity analysis of Ctrl-iNK cells and CD7 KO-CD7 CAR-iNK cells against Jurkat (**B**) or CCRF-CEM (**C**) tumor cells at the indicated E:T ratios after 4-h incubation. Data are represented as mean ± SD ($n = 4$). Mann-Whitney U test was used for statistics. ***$p < 0.001$. **D** Experimental design for the multiple rounds of tumor killing. The Ctrl-iNK and CD7 KO-CD7 CAR-iNK cells were respectively cocultured with Jurkat or CCRF-CEM tumor cells for 12 h per round at the E:T ratio of 1:1. Fresh tumor cells were added to the Ctrl-iNK/CD7 KO-CD7 CAR-iNK cell residues incubated every other 12 h. **E** Cytotoxicity analysis of three consecutive rounds of Jurkat cell killing by Ctrl-iNK or CD7 KO-CD7 CAR-iNK cells. Data are represented as mean ± SD ($n = 4$). Two-tailed independent *t*-test was used for statistics. ***p < 0.001. **F** Cytotoxicity analysis of three consecutive rounds of CCRF-CEM cell killing by Ctrl-iNK or CD7 KO-CD7 CAR-iNK cells. Data are represented as mean ± SD ($n = 4$). Two-tailed independent *t*-test was used for statistics. ***$p < 0.001$. **G-H** Assessment of CD107a expression by Ctrl-iNK or CD7 KO-CD7 CAR-iNK cells following 4 h of coculture with Jurkat/CCRF-CEM tumor cells at the ratio of 1:1. Data are represented as mean ± SD ($n = 3$). Two-tailed independent *t*-test was used for statistics. **$p < 0.01$, ***$p < 0.001$. **I-J** Measurement of IFN-γ production by Ctrl-iNK or CD7 KO-CD7 CAR-iNK cells in response to Jurkat/CCRF-CEM tumor cells. The Ctrl-iNK or CD7 KO-CD7 CAR-iNK cells were stimulated by Jurkat/CCRF-CEM at the ratio of 1:1 for 4 h. Data are represented as mean ± SD ($n = 3$). Two-tailed independent *t*-test was used for statistics. NS, not significant ($p > 0.05$), ***$p < 0.001$. **K-L** Evaluation of TNF-α production by Ctrl-iNK or CD7 KO-CD7 CAR-iNK cells in response to Jurkat/CCRF-CEM tumor cells. The Ctrl-iNK or CD7 KO-CD7 CAR-iNK cells were stimulated by Jurkat/CCRF-CEM at the ratio of 1:1 for 4 h. Data are represented as mean ± SD ($n = 3$). Two-tailed independent *t*-test was used for statistics. NS, not significant ($p > 0.05$), **$p < 0.01$

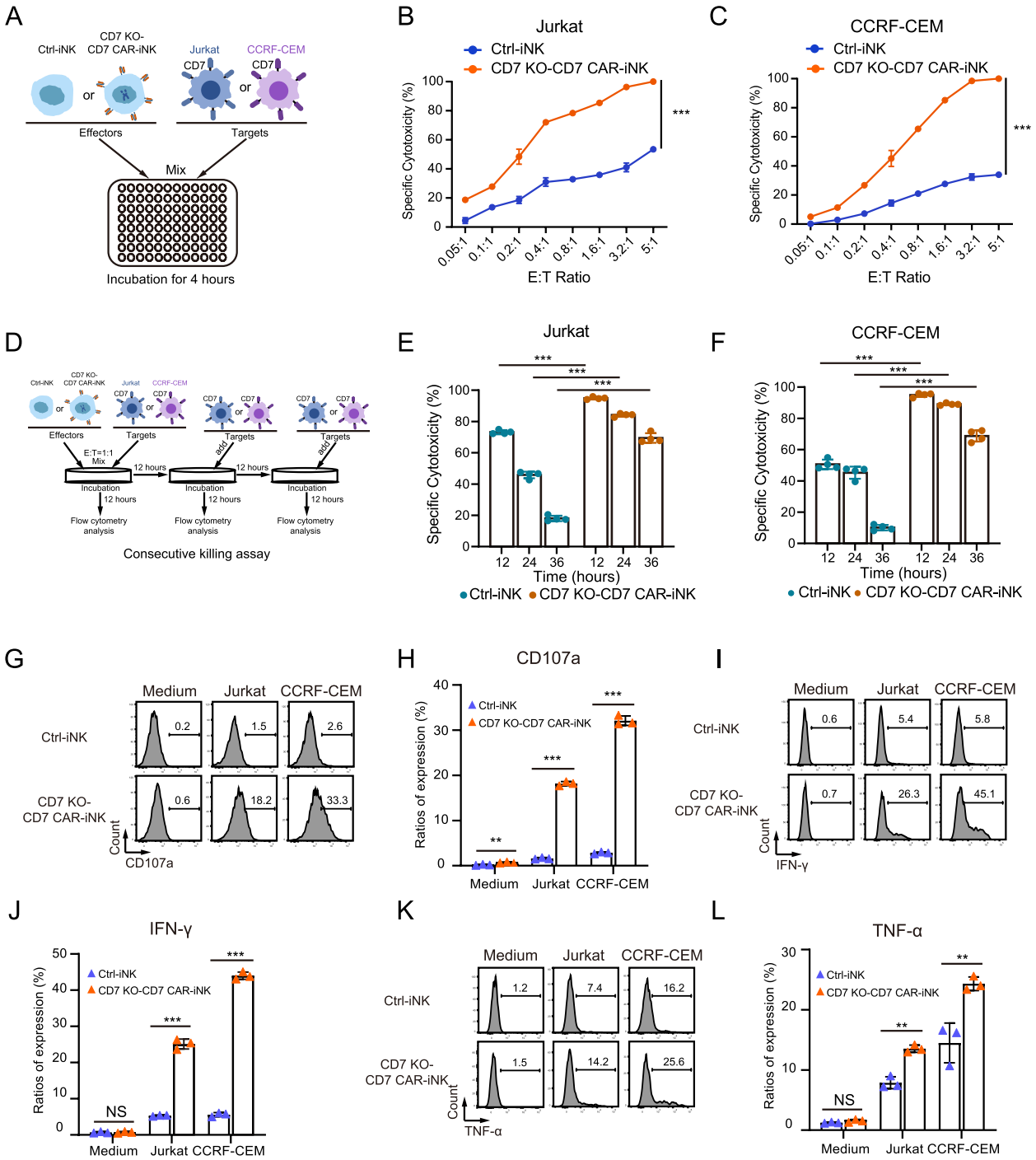

Fig. 3 (See legend on previous page.)

CXCR4 improves the bone marrow homing capacity and prolongs the persistence of CD7 KO-CD7 CAR-iNK cells in vivo

To promote the migration of hPSC-derived CD7 KO-CD7 CAR-iNK cells to the bone marrow and enhance their tumor-killing ability, we constructed CXCR4-overexpressing CD7 KO-CD7 CAR-hPSCs (CRO-CD7 CAR-hPSCs). To enable real-time in vivo tracking, the CRO-CD7 CAR-hPSCs were engineered to express luciferase (CRO-CD7 CAR-luci-hPSCs). Luciferase-expressing CD7 KO-CD7 CAR-hPSCs (CD7 KO-CD7 CAR-luci-hPSCs) were also constructed as

control (Fig. 5A). The CXCR4 and/or luciferase cassettes were integrated into the genomes of CD7 KO-CD7 CAR-hPSCs using the PiggyBac transposon system. The CXCR4 expression rates exceeded 98% in CRO-CD7 CAR-hPSCs and CRO-CD7 CAR-luci-hPSCs after two rounds of sorting (Fig. S4A). BLI and flow cytometry analysis verified the expression of luciferase in both CD7 KO-CD7 CAR-luci-hPSCs and CRO-CD7 CAR-luci-hPSCs (Fig. 5B, Fig. S4A). CRO-CD7 CAR-hPSCs, CD7 KO-CD7 CAR-luci-hPSCs, and CRO-CD7 CAR-luci-hPSCs were further differentiated into CRO-CD7 CAR-iNK, CD7 KO-CD7 CAR-luci-iNK, and CRO-CD7 CAR-luci-iNK cells using the organoid induction method. Flow cytometry analysis indicated the expression of CXCR4 in both CRO-CD7 CAR-iNK and CRO-CD7 CAR-luci-iNK cells (Fig. 5C). To assess their in vivo distribution and persistence, CD7 KO-CD7 CAR-luci-iNK and CRO-CD7 CAR-luci-iNK cells were injected via tail vein into B-NDG hIL15 mice on day 0. BLI and flow cytometry analysis were performed at designated time points to monitor the dynamic distribution and persistence of injected cells (Fig. 5D). BLI at the different time points post-injection revealed that both cell fractions were initially trapped predominantly in the lungs; however, after 24 h, they assumed different anatomical localizations. The CRO-CD7 CAR-luci-iNK cells could be maintained in vivo for more than 60 days (Fig. 5E and F). Flow cytometry analysis of the PB from iNK-injected B-NDG hIL15 mice showed that the proportion of injected huCD45$^+$ cells increased from about 0.6% at 7 days after injection to 11%—15% at 14 days after injection and then gradually decreased (Fig. 5G). Notably, the persistence of CRO-CD7 CAR-luci-iNK cells was significantly prolonged compared to the CD7 KO-CD7 CAR-luci-iNK group, which persisted for less than 28 days (Fig. 5E-G). To further confirm the homing sites of CD7 KO-CD7 CAR-luci-iNK and CRO-CD7 CAR-luci-iNK cells, we performed ex vivo BLI of the spine and flow cytometry analysis of the bone marrow cells from the lower extremities on day 1, day 10, day 21, and day 28 after injection of CD7 KO-CD7 CAR-luci-iNK or CRO-CD7 CAR-luci-iNK cells. The BLI indicated a significant fluorescence signal in the vertebrae from the CRO-CD7 CAR-luci-iNK group, while no fluorescence signal was detected in the vertebrae from the CD7 KO-CD7 CAR-luci-iNK group at the four time points (Fig. S4B). Flow cytometry analysis indicated that the CD7 KO-CD7 CAR-luci-iNK cells (huCD45$^+$CD56$^+$) emerged on day 10 (0.1% in bone marrow nuclear cells) and were undetectable on day 21. In contrast, the CRO-CD7 CAR-luci-iNK cells appeared as early as day 1 (0.1% in bone marrow nuclear cells) and peaked at 3.8% on day 10. Despite the decrease of CRO-CD7 CAR-luci-iNK cells in total bone marrow nuclear cells on day 21 (1.5%), we still observed 0.6% CRO-CD7 CAR-luci-iNK cells on day 28 (Fig. S4C). Taken together, these data indicate that CXCR4 overexpression enhances the homing capacity of CD7 KO-CD7 CAR-iNK cells to bone marrow compartments following adoptive transfer and extends their persistence in vivo.

CRO-CD7 CAR-iNK cells suppress the tumor progress in xenograft animals

To further assess the therapeutic effects of the CRO-CD7 CAR-iNK cells on tumor cells in vivo, we established the T-ALL xenograft animal models by transplanting the luciferase-expressing CCRF-CEM (CCRF-CEM-luci) cells into B-NDG hIL15 immune-deficient mice. The B-NDG hIL15 mice were injected with CCRF-CEM-luci tumor cells (1×10^5 cells/mouse) via tail vein on day 0 and received 1.0 Gy irradiation on day 1. Subsequently, Ctrl-iNK, CD7 KO-CD7 CAR-iNK, or CRO-CD7 CAR-iNK cells were intravenously injected into the tumor-bearing animals (1×10^7 cells/mouse) on day 1, day 4, and day 7, while phosphate-buffered saline (PBS) was intravenously injected as control. BLI was performed weekly to capture the kinetics of tumor growth (Fig. 6A). The vector copy number of CD7 CAR in CD7 KO-CD7 CAR-iNK cells was 1.58 ± 0.44 (mean ± SD), which had no difference

(See figure on next page.)

Fig. 4 Anti-tumor activity of CD7 KO-CD7 CAR-iNK cells against primary T-ALL cells. **A** Experimental design for the T-ALL patient tumor-killing assay by hPSC-derived CD7 KO-CD7 CAR-iNK cells. Mononuclear cells (MNCs) were first isolated from the bone marrow of patients with T-ALL and transplanted into B-NDG immunodeficient mice (1×10^6/mouse) via tail vein injection. Four weeks after transplantation, the proportion of primary tumor cells in the PB of B-NDG mice was monitored weekly using flow cytometry. Once the proportion of huCD45$^+$CD7$^+$ primary tumor cells exceeded 80% (approximately 6-9 weeks post-transplantation), the spleens of the B-NDG recipient mice were harvested and processed into single-cell suspensions. The resulting splenocytes were then cocultured with Ctrl-iNK or CD7 KO-CD7 CAR-iNK cells for tumor cytotoxicity assays. **B** Surface expression of CD7 in the splenic cells from B-NDG recipient mice measured by flow cytometry. **C-E** Cytotoxicity analysis of Ctrl-iNK or CD7 KO-CD7 CAR-iNK cells against T-ALL cells isolated from patient 1 (**C**), patient 2 (**D**), and patient 3 (**E**) at the indicated E:T ratios after 6-h incubation. Data are represented as mean ± SD ($n = 4$). Two-way ANOVA and Mann-Whitney U test were used for statistics. ***$p < 0.001$. **F–H** Cytotoxicity analysis of Ctrl-iNK or CD7 KO-CD7 CAR-iNK cells against T-ALL cells isolated from patient 1 (**F**), patient 2 (**G**), and patient 3 (**H**) at the E:T ratio of 1:2 after 3 h-, 6 h-, 9 h-, and 12 h- incubation. Data are represented as mean ± SD ($n = 4$). Two-way ANOVA and Mann-Whitney U test were used for statistics. ***$p < 0.001$

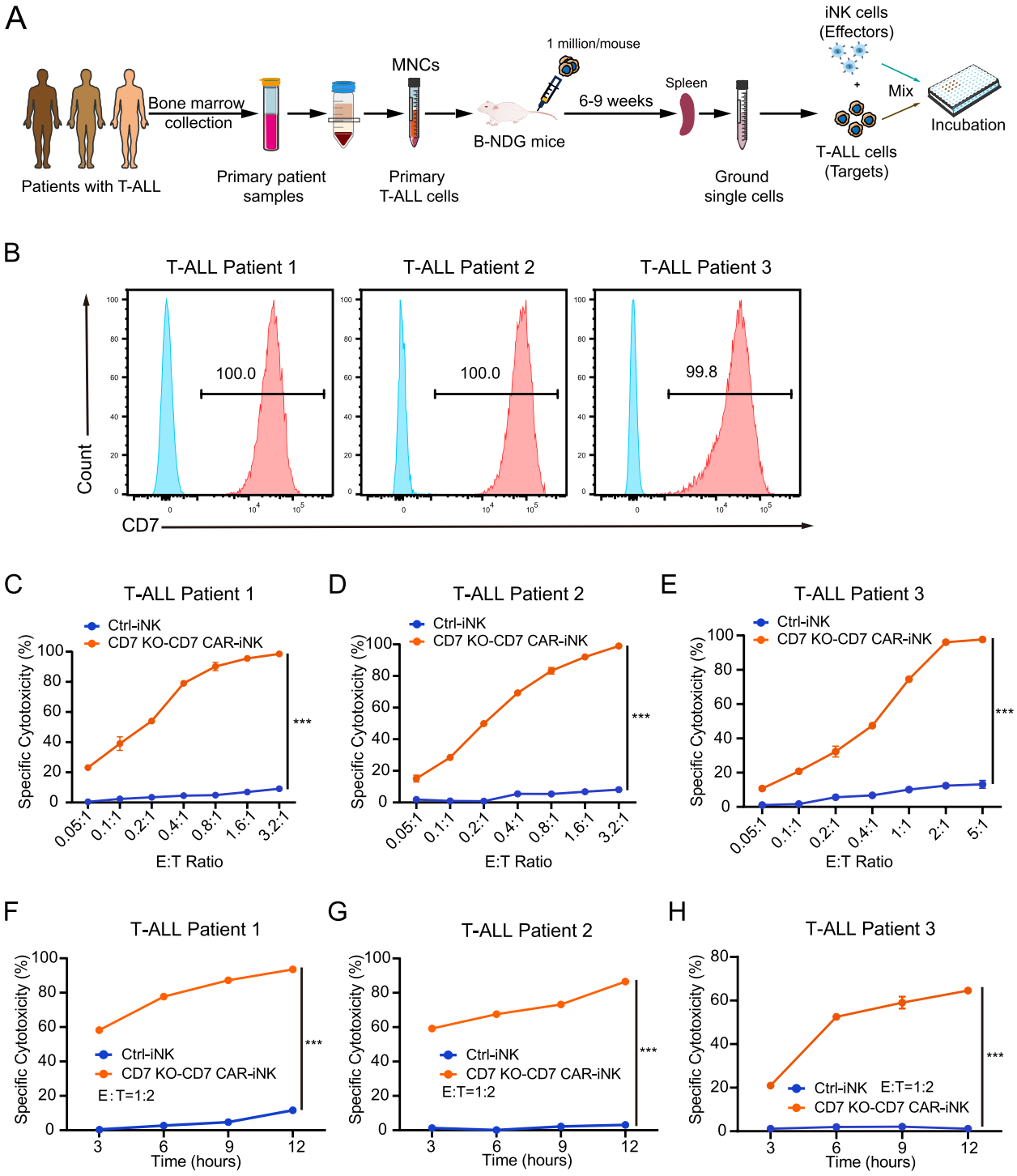

Fig. 4 (See legend on previous page.)

from that in CRO-CD7 CAR-iNK cells (1.81 ± 0.44, mean ± SD) (Fig. S5). The data showed that tumor burdens of the PBS group, Ctrl-iNK group, and CD7 KO-CD7 CAR-iNK group became increasingly severe, as indicated by the radiance and the value of total flux (Fig. 6B and C). Eventually, the PBS, Ctrl-iNK, and CD7 KO-CD7 CAR-iNK groups of mice needed ethical euthanasia due to the heavy tumor burden. However, the CRO-CD7 CAR-iNK cells showed stronger tumor-killing ability in xenograft animals with lower radiance and total flux measurements

(Fig. 6B and C). The CRO-CD7 CAR-iNK cell-treated mice survived significantly longer than the CD7 KO-CD7 CAR-iNK cell-treated mice, Ctrl-iNK cell-treated mice, and PBS-treated mice (Tumor + PBS: 29 days; Tumor + Ctrl-iNK: 30 days; Tumor + CD7 KO-CD7 CAR-iNK: 32 days; Tumor + CRO-CD7 CAR-iNK: 36 days; $p < 0.01$) (Fig. 6D). In conclusion, these results show that the CRO-CD7 CAR-iNK cells can efficiently suppress tumor development and prolong the survival of tumor-bearing mice, highlighting their potential as a therapeutic option for T-ALL treatment.

Discussion

In this study, we developed hPSC-derived CRO-CD7 CAR-iNK cells that avoid fratricide and show improved persistence in vivo. CD7 CAR-NK cells derived from UCB exhibited impaired expansion due to fratricide. By knocking out the *CD7* gene and ectopically expressing CD7 CAR in hPSCs, we successfully generated expandable and functional CD7 KO-CD7 CAR-iNK cells using an organoid culture method. These CD7 KO-CD7 CAR-iNK cells effectively avoided CD7-antigen-induced fratricide and exhibited robust cytotoxic activity against $CD7^+$ tumor cells in vitro, particularly primary tumor cells derived from T-ALL patients. Furthermore, CRO-CD7 CAR-iNK cells were generated from CXCR4-overexpressing CD7 KO-CD7 CAR-hPSCs to improve therapeutic efficacy. CXCR4 overexpression improved the bone marrow homing capacity and significantly prolonged the persistence of CRO-CD7 CAR-iNK cells in vivo. CRO-CD7 CAR-iNK effectively inhibited tumor progression in xenograft mice and significantly prolonged their survival. In the bone marrow, expression of IL-15 mRNA was considerably higher in CXCL12 (the ligand of CXCR4)-abundant reticular cells than in other marrow cells, and most NK cells were in contact with the processes of CXCL12-abundant reticular cells [38]. The B-NDG hIL15 mouse model used in this study is a substitution of endogenous mouse *Il15* gene locus with human *IL15* gene, which ensures the natural tissue-specific expression pattern of IL-15. We speculate that CXCR4 promotes the homing of injected CAR-iNK cells to the bone marrow microenvironment, wherein CAR-iNK cells have optimal conditions for survival and proliferation.

CD7 is expressed not only on T-cell malignancies and acute myeloid leukemia but also on most T cells and NK cells. Consequently, CAR-NK cells targeting CD7 would induce severe fratricide among themselves, leading to reduced proliferation and diminished therapeutic potential. Previous studies have proposed that one approach to overcome fratricide is to delete the *CD7* gene from T cells [39]. The absence of CD7 in CAR-T cells does not impair their functionality. Therefore, we adopted the CD7 knockout strategy to prevent fratricide in CD7 CAR-NK cells. Instead of performing gene editing at the mature T or NK cell stages [15, 40], we conducted the gene editing at the hPSC stage. NK cells generated from gene-modified hPSCs exhibited the advantages of homogeneity, higher gene editing efficiency, and lower costs of CAR engineering. The hESCs were provided by the Chinese National Stem Cell Resource Center, in compliance with the related ethics and national legislation of China. The CD7 KO-CD7 CAR-iNK cells exhibited comparable expansion ability and robust cytotoxic activity, indicating that the knockout of CD7 did not affect the development or function of hPSC-derived iNK cells.

Tissue-derived CAR-NK cells persisted in peripheral blood for less than 10–14 days after infusion [41]. The short persistence in vivo is also a key barrier for CAR-iNK cells derived from hPSCs in the clinical setting [42]. Enforced expression of exogenous CXCR4 in CD7 KO-CD7 CAR-iNK cells has extended the persistence of iNK cells in the PB of B-NDG hIL15 mice from 14 days to over 28 days when measured by flow cytometry analysis at the cellular level. Incorporation of IL-15 or IL-21 into the CRO-CD7 CAR-iNK cells may further increase their in vivo proliferation and persistence [20, 43]. A major concern of hPSC-based CAR-NK cell therapy is the risk of potential tumorigenicity caused by the undifferentiated hPSCs. Moreover, it is critical to generate large-scale CAR-iNK cells using a robust, reproducible, and GMP-compliant manufacturing process for future

(See figure on next page.)

Fig. 5 Dynamic analysis of CRO-CD7 CAR-iNK cells in the B-NDG hIL15 mice after injection. **A** Strategy for the construction of CXCR4-CD7 KO-CD7 CAR-hPSCs (CRO-CD7 CAR-hPSCs), CD7 KO-CD7 CAR-luciferase-hPSCs (CD7 KO-CD7 CAR-luci-hPSCs), and CXCR4-CD7 KO-CD7 CAR-luciferase-hPSCs (CRO-CD7 CAR-luci-hPSCs). **B** BLI images of the CD7 KO-CD7 CAR-luci-hPSCs and CRO-CD7 CAR-luci-hPSCs. **C** Representative flow cytometry plots of CRO-CD7 CAR-iNK, CD7 KO-CD7 CAR-luci-iNK, and CRO-CD7 CAR-luci-iNK cells on day 27. **D** Schematic diagram of in vivo studies with CD7 KO-CD7 CAR-luci-iNK and CRO-CD7 CAR-luci-iNK cells in B-NDG hIL15 mice. The CD7 KO-CD7 CAR-luci-iNK and CRO-CD7 CAR-luci-iNK cells were injected into B-NDG hIL15 mice (1×10^7 cells/mouse) via the tail vein on day 0, respectively. BLI and flow cytometry analysis were performed at the indicated time points. **E** BLI images showing the presence of CD7 KO-CD7 CAR-luci-iNK or CRO-CD7 CAR-luci-iNK cells in B-NDG hIL15 mice ($n = 2$ mice in each group) at the indicated time points. **F** Total flux (p/s) of the CD7 KO-CD7 CAR-luci-iNK or CRO-CD7 CAR-luci-iNK cells injected B-NDG hIL15 mice measured at the indicated time points ($n = 2$ mice in each group). **G** Flow cytometry analysis of CD7 KO-CD7 CAR-luci-iNK or CRO-CD7 CAR-luci-iNK cells in the PB of B-NDG hIL15 mice at the indicated time points

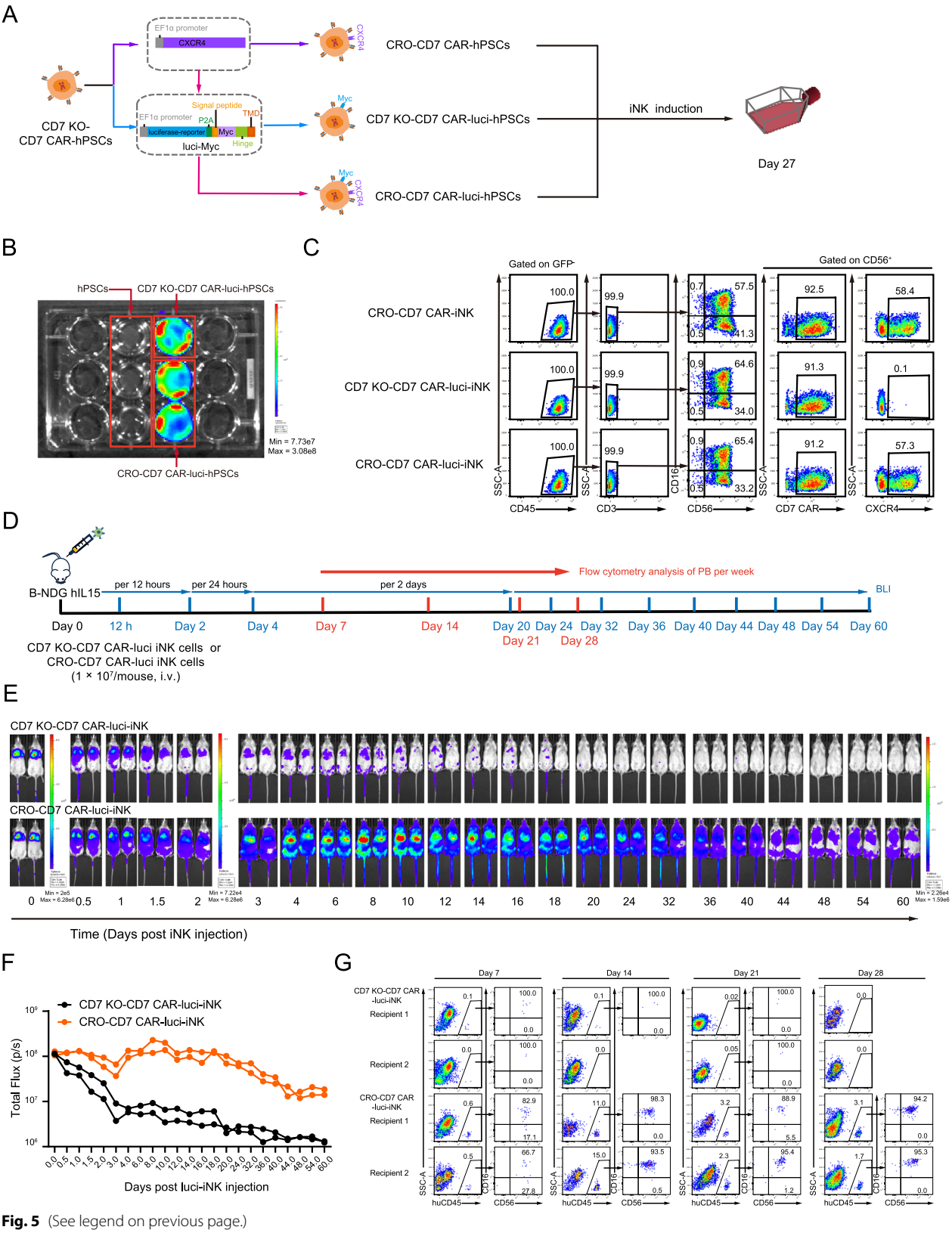

Fig. 5 (See legend on previous page.)

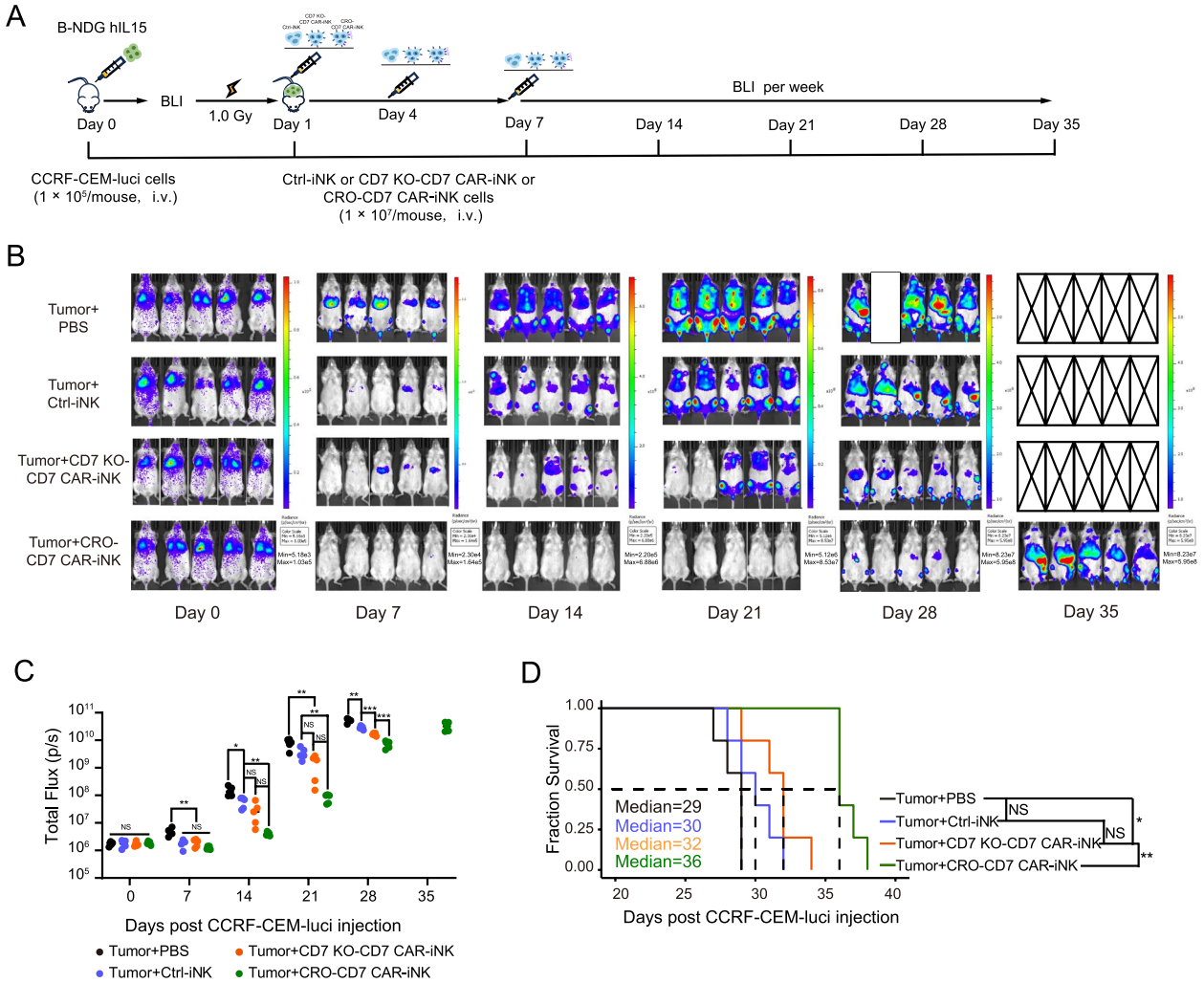

Fig. 6 Suppression of human T-cell leukemia progress in xenograft models by CRO-CD7 CAR-iNK cells. **A** Schematic diagram of in vivo studies with luciferase-expressing CCRF-CEM cells (CCRF-CEM-luci) in mouse xenograft models. The CCRF-CEM-luci tumor cells were injected into B-NDG hIL15 mice (1×10^5/mouse) via the tail vein on day 0. The mice were irradiated (1.0 Gy) on day 1. Equal numbers (1×10^7) of Ctrl-iNK, CD7 KO-CD7 CAR-iNK, or CRO-CD7 CAR-iNK cells were injected into each animal on day 1, day 4, and day 7. BLI was performed every week. **B** BLI images of the xenograft models at the indicated time points (Tumor + PBS, Tumor + Ctrl-iNK, Tumor + CD7 KO-CD7 CAR-iNK, and Tumor + CRO-CD7 CAR-iNK, $n = 5$ mice in each group). The radiance indicates tumor burden. **C** Total flux (p/s) of the xenograft models measured at the indicated time points ($n = 5$ mice in each group). Two-tailed independent *t*-test was used for statistics. NS, not significant ($p > 0.05$), *$p < 0.05$, **$p < 0.01$, ***$p < 0.001$. **D** Kaplan-Meier survival curves of the xenograft models ($n = 5$ mice in each group). Median survival: Tumor + PBS, 29 days; Tumor + Ctrl-iNK, 30 days; Tumor + CD7 KO-CD7 CAR-iNK, 32 days; Tumor + CRO-CD7 CAR-iNK, 36 days. The logarithmic rank (Mantel-Cox) test was used for statistics. NS, not significant, *$p < 0.05$, **$p < 0.01$

clinical applications of hPSC-derived CAR-iNK cells. A significant reduction in the cost of the CAR-iNK cell manufacturing to approximately $20,000 for each patient would offer an advantage over conventional CAR-T cell products, which reach $300,000 [44].

Recent advances in hPSC-derived CAR-iNK cells focus on improving their expansion, persistence, and anti-tumor activity. In previous research, mesothelin (MSLN) CAR-iNK cells were generated from hESCs and cryopreserved to mimic an off-the-shelf CAR-NK cell product [22]. The thawed MSLN CAR-iNK cells effectively eliminated the ovarian tumor cells. Moreover, hypoimmunogenic CD19 CAR-iNK cells derived from hESCs showed strong anti-tumor effects [23]. NK cells derived from engineered iPSCs expressing the high affinity FcγR fusion CD64/16A can be armed with antibody therapies targeting different tumor antigens, cryopreserved, thawed, and mediate ADCC in vitro and in vivo [45]. Another study showed that synNotch-engineered hPSC-derived NK cells are not only effective mediators of anti-glioblastoma

responses within the setting of CD73 and TIGIT/CD155 co-targeting, but also represent a powerful allogeneic treatment option for this tumor [46]. Disruption of TGF-β signaling pathway is required to mediate effective killing of hepatocellular carcinoma by human iPSC-derived NK cells [47]. The CAR-iNK cells have also been applied to clinical trials. Armin Ghobadi and colleagues reported a phase 1 trial evaluating the safety and maximum tolerated dose of iPSC-derived CAR NK cells (hereby referred to as FT596) in patients with relapsed or refractory B-cell lymphoma. FT596 was administered after conditioning chemotherapy. The results showed that FT596 was well tolerated, with no maximum tolerated dose identified. Although the trial was not designed to assess efficacy, there were encouraging responses to treatment [48].

CD7 CAR-T cells can be used to treat CD7-positive leukemias, including T-ALL, T-cell lymphoblastic lymphoma, and certain subtypes of acute myeloid leukemia [10, 14, 49, 50]. The CRO-CD7 CAR-iNK cells are capable of avoiding fratricide and demonstrating robust cytotoxic activity against $CD7^+$ tumor cells. These features make them highly promising for the treatment of the above-mentioned hematological malignancies. Recent research has also demonstrated that iPSC-derived CD70 CAR-NK cells, which selectively target activated $CD70^+$ T cells, offer a novel strategy for preventing allogeneic T cell rejection [51]. Similarly, CRO-CD7 CAR-iNK cells can target and deplete recipient $CD7^+$ T cells, thereby enhancing their in vivo persistence and therapeutic efficacy. Moreover, the infusion of CRO-CD7 CAR-iNK cells has potential applications in the treatment of T cell-mediated autoimmune diseases, such as type 1 diabetes and multiple sclerosis [52, 53], by selectively eliminating pathogenic T cells.

There are also some issues that need to be further explored. It is necessary to evaluate the safety of gene editing in hPSCs by detecting off-target integration sites before clinical trials. We found that CD7 KO-CD7 CAR-iNK cells exhibited a killing activity of 31%–38% against PBMCs at the E:T ratio of 0.8:1 (Fig. S6). Currently identified targets for treating T-cell malignancies, such as CD5 and CD7, are expressed not only in tumor cells but also in a proportion of healthy immune cells. It is very challenging to avoid the killing of normal CD5 or CD7 positive T cells and NK cells when using these targets for CAR-T or CAR-NK immunotherapy. A previous study has established CD7 KO-HSCs by knocking out the CD7 molecule in hematopoietic stem cells, which can differentiate into T and NK cells lacking CD7 expression after being transplanted into immunodeficient mice. These CD7-KO T and NK cells resist CD7 CAR-T attack, preserving host immunity post-CAR-T treatment [54]. Nonetheless, our strategy of generating CRO-CD7 CAR-iNK cells from hPSCs offers an option for off-the-shelf cell products for treating $CD7^+$ T-ALL.

Despite significant progress in treating T-ALL, long-term suppression of tumor progression remains a challenge, with few drugs or treatments achieving durable efficacy [55]. CXCR4 can significantly enhance the in vivo distribution and improve the persistence of iNK cells, thus enhancing the anti-tumor ability [56]. We have previously reported that CXCR4-expressing NK progenitor cells derived from hPSCs can effectively eliminate minimal residual disease in tumor models [30]. Therefore, combining CD7 CAR-iNK progenitor cells with chemotherapeutic drugs holds promise for effectively eliminating minimal residual disease in T-ALL models.

Conclusions

In conclusion, CRO-CD7 CAR-iNK cells derived from hPSCs avoid fratricide and exhibit improved persistence and robust anti-tumor abilities in vivo. This study offers insights into the clinical potential of hPSC-derived CD7 CAR-iNK cells for the treatment of T-cell malignancies.

Abbreviations

hPSCs	Human pluripotent stem cells
T-ALL	T-cell acute lymphoblastic leukemia
UCB	Umbilical cord blood
CAR	Chimeric antigen receptor
CD7 KO-hPSC	CD7 knockout hPSCs
CD7 KO-iNK	CD7 knockout iNK
CD7 KO-CD7 CAR-hPSCs	CD7 CAR-expressing CD7 KO-hPSCs
CD7 KO-CD7 CAR-iNK	CD7 CAR-expressing CD7 KO-iNK
CRO-CD7 CAR-hPSCs	CXCR4-expressing CD7 KO-CD7 CAR-hPSCs
CRO-CD7 CAR-iNK	CXCR4-expressing CD7 KO-CD7 CAR-iNK
CD7 KO-CD7 CAR-luci-hPSCs	CD7 KO-CD7 CAR-luciferase-hPSCs
CRO-CD7 CAR-luci-hPSCs	CXCR4-CD7 KO-CD7 CAR-luciferase-hPSCs
CD7 KO-CD7 CAR-luci-iNK	CD7 KO-CD7 CAR-luciferase-iNK
CRO-CD7 CAR-luci-iNK	CXCR4-CD7 KO-CD7 CAR-luciferase-iNK
B-NDG	NOD.CB17-*Prkdc*^{scid}*Il2rg*^{tm1Bcgen}/Bcgen
B-NDG hIL15	NOD.CB17-*Prkdc*^{scid} *Il2rg*^{tm1Bcgen} *Il15*$^{tm1(IL15)Bcgen}$/Bcgen
scFv	Single-chain variable fragment
MNCs	Mononuclear cells
E:T ratio	Effector:Target ratio
IFN-γ	Interferon γ
TNF-α	Tumor necrosis factor α
NK	Natural killer
PB	Peripheral blood
BLI	Bioluminescence imaging
PBS	Phosphate-buffered saline

Supplementary Information

The online version contains supplementary material available at https://doi.org/10.1186/s13045-025-01712-3.

Supplementary Material 1

Acknowledgements
We thank members of our team for critical discussion and suggestions.

Authors' contributions
Y.Q.L. designed and conducted all experiments, performed data analysis and wrote the manuscript. Z.Y.X. performed the core experiments; X.J.Z., C.Y.Z., and F.X.H. performed multiple experiments; Y.W., Y.H.L., H.D.H., Z.Q.W., C.X.X., Q.T.W., L.Q.Z., Y.Q.Z., H.M.Q., Y.Y.S., Y.C., F.Z., J.X.W., P.C.L., J.C.X., L.J.L., and Y.P.Z. assisted in completing the experiments. J.L.Z., W.B.Q., A.B.L., X.F.Z., F.X.H., T.J.W., M.Y.Z., and J.Y.W. discussed the data; T.J.W., M.Y.Z. and J.Y.W. wrote the manuscript; and J.Y.W. designed the project and provided final approval of the manuscript.

Funding
This work was supported by the National Key R&D Program of China (2024YFA1108302, 2021YFA1100800), the National Natural Science Foundation of China (81925002, 82450001, 82470120, 82300132, 32300676, 82350104), the R&D program of Beijing Escure Biotechnology Co., Ltd. (E441O71131), and the Noncommunicable Chronic Diseases-National Science and Technology Major Project (No. 2023ZD0501200).

Data availability
No datasets were generated or analysed during the current study.

Declarations

Ethics approval and consent to participate
Experiments and handling of mice were conducted under the Institutional Animal Care and Use Committee of the Institute of Zoology, Chinese Academy of Sciences. The studies involving humans were approved by the Biomedical Research Ethics Committee of the Institute of Zoology, Chinese Academy of Sciences. The use of patient samples was conducted in accordance with the provisions of the Declaration of Helsinki. All patient samples were collected with priori patient consent signatures and were reviewed and approved by the Ethics Committee of State Key Laboratory of Experimental Hematology, Institute of Hematology and Blood Disease Hospital, Chinese Academy of Medical Sciences and Peking Union Medical College.

Consent for publication
Not applicable.

Competing interests
The authors declare no competing interests.

Author details
[1]State Key Laboratory of Organ Regeneration and Reconstruction, Institute of Zoology, Chinese Academy of Sciences, Beijing 100101, China. [2]University of Chinese Academy of Sciences, Beijing 100049, China. [3]Beijing Institute for Stem Cell and Regenerative Medicine, Beijing 100101, China. [4]State Key Laboratory of Experimental Hematology, National Clinical Research Center for Blood Diseases, Haihe Laboratory of Cell Ecosystem, Institute of Hematology & Blood Diseases Hospital, Chinese Academy of Medical Sciences & Peking Union Medical College, Tianjin 300020, China. [5]Department of Hematology, the Second Affiliated Hospital, College of Medicine, Zhejiang University, Hangzhou, Zhejiang 310009, China. [6]Department of Hematology, Tongji Hospital of Tongji University, Shanghai 200065, China.

Received: 23 January 2025 Accepted: 9 May 2025
Published online: 19 May 2025

References

1. Litzow MR, Ferrando AA. How I treat T-cell acute lymphoblastic leukemia in adults. Blood. 2015;126:833–41.
2. Marks DI, et al. T-cell acute lymphoblastic leukemia in adults: clinical features, immunophenotype, cytogenetics, and outcome from the large randomized prospective trial (UKALL XII/ECOG 2993). Blood. 2009;114:5136–45.
3. Marks DI, Rowntree C. Management of adults with T-cell lymphoblastic leukemia. Blood. 2017;129:1134–42.
4. Park JH, et al. Long-Term Follow-up of CD19 CAR Therapy in Acute Lymphoblastic Leukemia. N Engl J Med. 2018;378:449–59.
5. Raje N, et al. Anti-BCMA CAR T-Cell Therapy bb2121 in Relapsed or Refractory Multiple Myeloma. N Engl J Med. 2019;380:1726–37.
6. Rabinowich H, Pricop L, Herberman RB, Whiteside TL. Expression and function of CD7 molecule on human natural killer cells. J Immunol. 1994;152:517–26.
7. Ware RE, Scearce RM, Dietz MA, Starmer CF, Palker TJ, Haynes BF. Characterization of the surface topography and putative tertiary structure of the human CD7 molecule. J Immunol. 1989;143:3632–40.
8. Campana D, van Dongen JJ, Mehta A, Coustan-Smith E, Wolvers-Tettero IL, Ganeshaguru K, Janossy G. Stages of T-cell receptor protein expression in T-cell acute lymphoblastic leukemia. Blood. 1991;77:1546–54.
9. Bayon-Calderon F, Toribio ML, Gonzalez-Garcia S. Facts and Challenges in Immunotherapy for T-Cell Acute Lymphoblastic Leukemia. Int J Mol Sci. 2020;21:7685.
10. Pan J, et al. Donor-Derived CD7 Chimeric Antigen Receptor T Cells for T-Cell Acute Lymphoblastic Leukemia: First-in-Human. Phase I Trial J Clin Oncol. 2021;39:3340–51.
11. Teachey DT, Hunger SP. Anti-CD7 CAR T cells for T-ALL: impressive early-stage efficacy. Nat Rev Clin Oncol. 2021;18:677–8.
12. Gomes-Silva D, Srinivasan M, Sharma S, Lee CM, Wagner DL, Davis TH, Rouce RH, Bao G, Brenner MK, Mamonkin M. CD7-edited T cells expressing a CD7-specific CAR for the therapy of T-cell malignancies. Blood. 2017;130:285–96.
13. Georgiadis C, Rasaiyaah J, Gkazi SA, Preece R, Etuk A, Christi A, Qasim W. Base-edited CAR T cells for combinational therapy against T cell malignancies. Leukemia. 2021;35:3466–81.
14. Gomes-Silva D, et al. CD7 CAR T Cells for the Therapy of Acute Myeloid Leukemia. Mol Ther. 2019;27:272–80.
15. Jiang J, Chen J, Liao C, Duan Y, Wang Y, Shang K, Huang Y, Tang Y, Gao X, Gu Y, Sun J. Inserting EF1alpha-driven CD7-specific CAR at CD7 locus reduces fratricide and enhances tumor rejection. Leukemia. 2023;37:1660–70.
16. Li S, et al. CD7 targeted "off-the-shelf" CAR-T demonstrates robust in vivo expansion and high efficacy in the treatment of patients with relapsed and refractory T cell malignancies. Leukemia. 2023;37:2176–86.
17. Png YT, Vinanica N, Kamiya T, Shimasaki N, Coustan-Smith E, Campana D. Blockade of CD7 expression in T cells for effective chimeric antigen receptor targeting of T-cell malignancies. Blood Adv. 2017;1:2348–60.
18. Dagher OK, Posey AD Jr. Forks in the road for CAR T and CAR NK cell cancer therapies. Nat Immunol. 2023;24:1994–2007.
19. Pappas JJ, Yang PC. Human ESC vs iPSC-pros and cons. J Cardiovasc Transl Res. 2008;1:96–9.
20. Cichocki F, et al. Dual antigen-targeted off-the-shelf NK cells show durable response and prevent antigen escape in lymphoma and leukemia. Blood. 2022;140:2451–62.
21. Li Y, Hermanson DL, Moriarity BS, Kaufman DS. Human iPSC-Derived Natural Killer Cells Engineered with Chimeric Antigen Receptors Enhance Anti-tumor Activity. Cell Stem Cell. 2018;23(181–192): e185.
22. Liu Y, et al. Mesothelin CAR-engineered NK cells derived from human embryonic stem cells suppress the progression of human ovarian cancer in animals. Cell Prolif. 2024;57: e13727.
23. Zhang Q, et al. Hypoimmunogenic CD19 CAR-NK cells derived from embryonic stem cells suppress the progression of human B-cell malignancies in xenograft animals. Front Immunol. 2024;15:1504459.
24. Sabbah M, Jondreville L, Lacan C, Norol F, Vieillard V, Roos-Weil D, Nguyen S. CAR-NK Cells: A Chimeric Hope or a Promising Therapy? Cancers (Basel). 2022;14:3839.
25. Beider K, et al. Involvement of CXCR4 and IL-2 in the homing and retention of human NK and NK T cells to the bone marrow and spleen of NOD/SCID mice. Blood. 2003;102:1951–8.
26. Levy E, Reger R, Segerberg F, Lambert M, Leijonhufvud C, Baumer Y, Carlsten M, Childs R. Enhanced Bone Marrow Homing of Natural Killer Cells Following mRNA Transfection With Gain-of-Function Variant CXCR4(R334X). Front Immunol. 2019;10:1262.
27. Moles MW, et al. CXCR4 has a dual role in improving the efficacy of BCMA-redirected CAR-NK cells in multiple myeloma. Front Immunol. 2024;15:1383136.
28. Muller N, Michen S, Tietze S, Topfer K, Schulte A, Lamszus K, Schmitz M, Schackert G, Pastan I, Temme A. Engineering NK Cells Modified With an EGFRvIII-specific Chimeric Antigen Receptor to Overexpress CXCR4

Improves Immunotherapy of CXCL12/SDF-1alpha-secreting Glioblastoma. J Immunother. 2015;38:197–210.
29. Ng YY, Du Z, Zhang X, Chng WJ, Wang S. CXCR4 and anti-BCMA CAR co-modified natural killer cells suppress multiple myeloma progression in a xenograft mouse model. Cancer Gene Ther. 2022;29:475–83.
30. Wang Z, et al. Pluripotent stem cell-derived NK progenitor cell therapy prevents tumour occurrence and eradicates minimal residual disease. 2025. https://doi.org/10.1101/2025.01.07.631650.
31. Baum W, Steininger H, Bair HJ, Becker W, Hansen-Hagge TE, Kressel M, Kremmer E, Kalden JR, Gramatzki M. Therapy with CD7 monoclonal antibody TH-69 is highly effective for xenografted human T-cell ALL. Br J Haematol. 1996;95:327–38.
32. Riviere I, Brose K, Mulligan RC. Effects of retroviral vector design on expression of human adenosine deaminase in murine bone marrow transplant recipients engrafted with genetically modified cells. Proc Natl Acad Sci U S A. 1995;92:6733–7.
33. Wang Y, et al. Comparison of seven CD19 CAR designs in engineering NK cells for enhancing anti-tumour activity. Cell Prolif. 2024;57: e13683.
34. Chen Y, Hu Y, Wang X, Luo S, Yang N, Chen Y, Li Z, Zhou Q, Li W. Synergistic engineering of CRISPR-Cas nucleases enables robust mammalian genome editing. Innovation (Camb). 2022;3: 100264.
35. Huang D, et al. Lateral plate mesoderm cell-based organoid system for NK cell regeneration from human pluripotent stem cells. Cell Discov. 2022;8:121.
36. Cichocki F, Miller JS. In vitro development of human Killer-Immunoglobulin Receptor-positive NK cells. Methods Mol Biol. 2010;612:15–26.
37. Haderbache R, et al. Droplet digital PCR allows vector copy number assessment and monitoring of experimental CAR T cells in murine xenograft models or approved CD19 CAR T cell-treated patients. J Transl Med. 2021;19:265.
38. Noda M, Omatsu Y, Sugiyama T, Oishi S, Fujii N, Nagasawa T. CXCL12-CXCR4 chemokine signaling is essential for NK-cell development in adult mice. Blood. 2011;117:451–8.
39. Liu J, Zhang Y, Guo R, Zhao Y, Sun R, Guo S, Lu W, Zhao M. Targeted CD7 CAR T-cells for treatment of T-Lymphocyte leukemia and lymphoma and acute myeloid leukemia: recent advances. Front Immunol. 2023;14:1170968.
40. You F, Wang Y, Jiang L, Zhu X, Chen D, Yuan L, An G, Meng H, Yang L. A novel CD7 chimeric antigen receptor-modified NK-92MI cell line targeting T-cell acute lymphoblastic leukemia. Am J Cancer Res. 2019;9:64–78.
41. Lei W, et al. Safety and feasibility of 4–1BB co-stimulated CD19-specific CAR-NK cell therapy in refractory/relapsed large B cell lymphoma: a phase 1 trial. Nat Cancer. 2025. https://doi.org/10.1038/s43018-025-00940-3.
42. Shapiro RM, Romee R. iPSC-derived CD19 CAR NK cells for relapsed or refractory lymphoma. Lancet. 2025;405:98–9.
43. Zhang Y, Zhang C, He M, Xing W, Hou R, Zhang H. Co-expression of IL-21-Enhanced NKG2D CAR-NK cell therapy for lung cancer. BMC Cancer. 2024;24:119.
44. Lin X, Sun Y, Dong X, Liu Z, Sugimura R, Xie G. IPSC-derived CAR-NK cells for cancer immunotherapy. Biomed Pharmacother. 2023;165: 115123.
45. Snyder KM, et al. iPSC-derived natural killer cells expressing the FcgammaR fusion CD64/16A can be armed with antibodies for multitumor antigen targeting. J Immunother Cancer. 2023;11:e007280.
46. Lupo KB, Yao X, Borde S, Wang J, Torregrosa-Allen S, Elzey BD, Utturkar S, Lanman NA, McIntosh M, Matosevic S. synNotch-programmed iPSC-derived NK cells usurp TIGIT and CD73 activities for glioblastoma therapy. Nat Commun. 2024;15:1909.
47. Thangaraj JL, Coffey M, Lopez E, Kaufman DS. Disruption of TGF-beta signaling pathway is required to mediate effective killing of hepatocellular carcinoma by human iPSC-derived NK cells. Cell Stem Cell. 2024;31(1327–1343): e1325.
48. Ghobadi A, et al. Induced pluripotent stem-cell-derived CD19-directed chimeric antigen receptor natural killer cells in B-cell lymphoma: a phase 1, first-in-human trial. Lancet. 2025;405:127–36.
49. Hu Y, et al. Genetically modified CD7-targeting allogeneic CAR-T cell therapy with enhanced efficacy for relapsed/refractory CD7-positive hematological malignancies: a phase I clinical study. Cell Res. 2022;32:995–1007.
50. Lu P, Liu Y, Yang J, Zhang X, Yang X, Wang H, Wang L, Wang Q, Jin D, Li J, Huang X. Naturally selected CD7 CAR-T therapy without genetic manipulations for T-ALL/LBL: first-in-human phase 1 clinical trial. Blood. 2022;140:321–34.
51. Wang L, et al. CD70-targeted iPSC-derived CAR-NK cells display potent function against tumors and alloreactive T cells. Cell Rep Med. 2024;6:101889.
52. Gearty SV, et al. An autoimmune stem-like CD8 T cell population drives type 1 diabetes. Nature. 2022;602:156–61.
53. Zhao Y, Zhang J, Cheng X, Huang W, Shen S, Wu S, Huang Y, Nie G, Wang H, Qiu W. Targeting L-Selectin Lymphocytes to Deliver Immunosuppressive Drug in Lymph Nodes for Durable Multiple Sclerosis Treatment. Adv Sci (Weinh). 2023;10: e2300738.
54. Kim MY, Cooper ML, Jacobs MT, Ritchey JK, Hollaway J, Fehniger TA, DiPersio JF. CD7-deleted hematopoietic stem cells can restore immunity after CAR T cell therapy. JCI Insight. 2021;6:e149819.
55. Polonen P, Mullighan CG, Teachey DT. Classification and risk stratification in T-lineage acute lymphoblastic leukemia. Blood. 2024;145:1464–74.
56. Millar HJ, et al. CXCR4 transgene improves in vivo migration and efficacy of engineered iPSC-derived natural killer cells. Cancer Research. 2024;84:6802.

Publisher's Note